nature chemical biology

ARTICLE

PUBLISHED ONLINE: 27 JULY 2015 | DOI: 10.1038/NCHEMBIO.1869

# Tunable and reversible drug control of protein production via a self-excising degron

Hokyung K Chung[1], Conor L Jacobs[1], Yunwen Huo[2], Jin Yang[3], Stefanie A Krumm[4], Richard K Plemper[4,5], Roger Y Tsien[3,6,7] & Michael Z Lin[2,8]*

**An effective method for direct chemical control over the production of specific proteins would be widely useful. We describe small molecule–assisted shutoff (SMASh), a technique in which proteins are fused to a degron that removes itself in the absence of drug, resulting in the production of an untagged protein. Clinically tested HCV protease inhibitors can then block degron removal, inducing rapid degradation of subsequently synthesized copies of the protein. SMASh allows reversible and dose-dependent shutoff of various proteins in multiple mammalian cell types and in yeast. We also used SMASh to confer drug responsiveness onto an RNA virus for which no licensed inhibitors exist. As SMASh does not require the permanent fusion of a large domain, it should be useful when control over protein production with minimal structural modification is desired. Furthermore, as SMASh involves only a single genetic modification and does not rely on modulating protein-protein interactions, it should be easy to generalize to multiple biological contexts.**



Technology for rapidly shutting off the production of specific proteins in eukaryotes would be widely useful in research and in gene and cell therapies, but a simple and effective method has yet to be developed. Controlling protein production through repression of transcription is slow in onset because previously transcribed mRNA molecules continue to produce proteins. RNA interference (RNAi) induces mRNA destruction, but RNAi is often only partially effective and can exhibit both sequence-independent and sequence-dependent off-target effects[1]. Furthermore, mRNA and protein abundance are not always correlated as a result of the translational regulation of specific mRNAs[2–4]. Lastly, both transcriptional repression and RNAi take days to reverse[5,6].

To address these limitations, we wished to devise a method for chemical regulation of protein expression at the post-translational level. An ideal method would feature (i) genetic specification of the target protein, (ii) a single genetic modification for simplicity, (iii) minimal modification of the expressed protein, (iv) generalizability to many proteins and cell types and (v) control by a drug with proven safety and bioavailability in mammals. While methods have been devised with some of these characteristics (**Supplementary Results**, **Supplementary Table 1**), none have encompassed all of them. We envisioned that a degron that removes itself in a drug-controllable manner could serve as the basis for a new method with all of the desired features. In particular, we reasoned that if a site-specific, drug-inhibitable protease and a degron were fused to a protein via an intervening protease site, then by default the protease and degron would be removed and the protein expressed. However, in the presence of protease inhibitor, the degron would remain attached on new protein copies and cause their rapid degradation (**Fig. 1a**).

Here we show a system of this design using the hepatitis C virus (HCV) nonstructural protein 3 (NS3) protease enables clinically tested drugs to effectively shut off protein expression, in a method we have termed 'small molecule–assisted shutoff,' or SMASh. SMASh enabled drug-induced suppression of various proteins in multiple eukaryotic cell types. In contrast to other single-component methods for the post-translational regulation of protein expression, SMASh functioned robustly in yeast as well. Finally, we used SMASh to confer HCV protease–inhibitor sensitivity onto an RNA virus currently in clinical trials for cancer, but for which no licensed drug inhibitor exists. SMASh thus enables post-translational regulation of protein production with rapid onset and minimal protein modification in a broad array of experimental systems and requires only a single genetic modification, the addition of the SMASh tag to the coding sequence of interest.

## RESULTS

### The SMASh tag, a drug-controllable self-removing degron

We previously used the HCV NS3 protease to control protein tagging with drugs[7,8] because it is monomeric, highly selective and well inhibited by nontoxic cell-permeable inhibitors such as simeprevir, danoprevir, asunaprevir and ciluprevir, some of which are clinically available[9–12]. We hypothesized that we could use NS3 protease fused in *cis* to remove degrons, by default, from proteins of interest shortly after their translation, and then apply inhibitor to block degron removal on subsequently synthesized copies. If the degron were sufficiently strong, then presence of the inhibitor would cause newly synthesized proteins to be rapidly degraded, which would, in effect, shut off further protein production (**Fig. 1a**).

During the development of tags for newly synthesized proteins, called TimeSTAMPs[7], we cloned a sequence encoding the NS3 protease domain (hereafter referred to as NS3pro) followed by the HCV NS4A protein (**Fig. 1b**). We noticed that expression (in HEK293 cells) of a mouse PSD95 protein variant, in which the mouse PSD95 protein was connected to NS3pro via an NS3 substrate sequence, occurred both when self-removal of NS3pro was allowed to take place in the absence of drug and when removal was inhibited by asunaprevir (**Fig. 1c**). However, when PSD95 was fused via the same substrate sequence to NS3pro followed by NS4A, it was

[1]Department of Biology, Stanford University, Stanford, California, USA. [2]Department of Pediatrics, Stanford University, Stanford, California, USA. [3]Department of Pharmacology, University of California, San Diego, La Jolla, California, USA. [4]Department of Pediatrics, Emory University, Atlanta, Georgia, USA. [5]Institute for Biomedical Sciences, Georgia State University, Atlanta, Georgia, USA. [6]Department of Chemistry and Biochemistry, University of California, San Diego, La Jolla, California, USA. [7]Howard Hughes Medical Institute, University of California, San Diego, La Jolla, California, USA. [8]Department of Bioengineering, Stanford University, Stanford, California, USA. *e-mail: mzlin@stanford.edu

expressed well in the absence but not the presence of asunaprevir (**Fig. 1c**).

To explain these results, we surmised that the arrangement of the NS3pro and NS4A sequences in our construct had created a functional degron. During HCV replication, the free NS4A N terminus forms a hydrophobic α-helix that is inserted into the endoplasmic reticulum membrane[13] (**Supplementary Fig. 1a**). This N terminus is created by cleavage of the HCV nonstructural polypeptide at the NS3-4A junction (**Supplementary Fig. 1a**) because it is positioned in the protease active site by the NS3 helicase domain[14]. As our engineered construct lacks the helicase domain, NS3-4A cleavage might not occur (**Supplementary Fig. 1b**), and the hydrophobic sequences of NS4A, unable to insert into the membrane without a free N terminus, might then exhibit degron-like activity.

We tested the roles of these putative destabilizing elements in suppressing the expression of jellyfish yellow fluorescent protein (YFP) that was fused to the self-removing NS3pro-NS4A cassette. In the absence of asunaprevir, a 30-kDa YFP fragment was released as expected (**Fig. 1d**). In contrast, in the presence of asunaprevir, virtually no full-length 64-kDa YFP–NS3pro-NS4A fusion protein was detected (**Fig. 1d**), results that were similar to those with PSD95. Mutation of a 41-residue stretch, comprising a putatively unstructured sequence from NS3 helicase and a hydrophobic sequence from NS4A (dotted line in **Fig. 1b**), to glycines and serines (referred to as the 'GGS' variant) rescued expression of the full-length protein in the presence of the drug to levels similar to those seen for YFP expression without drug (**Fig. 1d**). These results indicated that an unstructured hydrophobic sequence derived from NS3 helicase and NS4A triggers rapid degradation of the fusion protein.

We next examined which proteolytic pathways were responsible for degrading the NS3pro-NS4A fusion proteins. We assayed the expression of uncleaved YFP–NS3pro-NS4A in HeLa cells treated with asunaprevir and various proteasome or autophagy-pathway inhibitors (**Supplementary Fig. 1c**). Inhibition of either the proteasome (with MG132 or bortezomib) or the autophagy pathway (with chloroquine or bafilomycin A1) modestly increased YFP–NS3pro-NS4A protein levels (**Supplementary Fig. 1c**). However, the combined inhibition of proteasome activity and autophagolysosome formation (by treatment with MG132 and chloroquine) rescued YFP–NS3pro-NS4A expression to the same level as that seen for the GGS variant (**Supplementary Fig. 1c**). This was not restricted to YFP fusions, as a PSD95–NS3pro-NS4A fusion was similarly affected (**Supplementary Fig. 1d**). These findings suggest that the NS3pro-NS4A cassette harbors a bifunctional degron capable of both proteasomal and lysosomal degradation.

To summarize our results so far, proteins fused to the NS3 protease–NS4A cassette via an NS3 substrate sequence were expressed well in the absence of an NS3 protease inhibitor and were present at the size expected for the untagged, released proteins. By contrast, in the presence of the NS3 protease inhibitor, steady-state levels of the fusion proteins were drastically reduced. This implies that fusion of a target protein with the NS3pro-NS4A cassette,

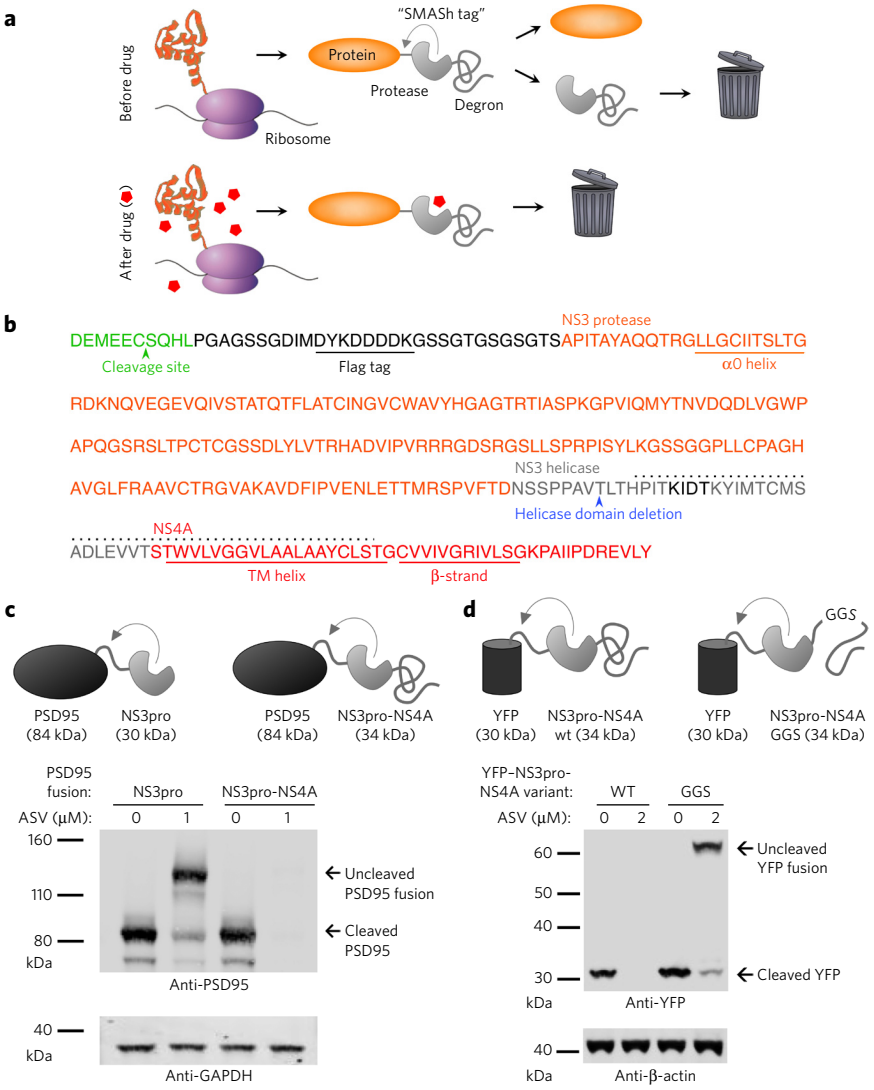


**Figure 1 | Small molecule-assisted shutoff (SMASh) concept and development.** (**a**) SMASh concept. Top, a target protein is fused to the SMASh tag via an HCV NS3 protease-recognition site. After protein folding, the SMASh tag is removed by its internal protease activity and is degraded due to internal degron activity. Bottom, addition of a protease inhibitor induces the rapid degradation of subsequently synthesized copies of the tagged protein, effectively shutting off further protein production. (**b**) Amino acid sequence of the SMASh tag. Sequences derived from the NS3 protease domain (orange), the NS3 helicase domain (gray), and the NS4A protein (red) are shown. Secondary structures in the context of the original HCV polyprotein are underlined. The NS4A-4B protease substrate (green) has an arrow indicating site of cleavage. Dotted line indicates putative degron region. TM, transmembrane. (**c**) Top, schematic showing the organization of PSD95 fusions with NS3 protease (NS3pro) or NS3pro-NS4A, with predicted protein-fragment sizes indicated. Bottom, immunoblots for PSD95 in the absence or presence of the protease inhibitor asunaprevir (ASV). PSD95 was detectable in HEK293 lysates 24 h post-transfection, for both constructs. GAPDH served as a loading control. (**d**) A specific element within NS3pro-NS4A is necessary for degron activity. Top, schematic showing the organization of YFP fusions with wild-type NS3pro-NS4A (WT) or the GGS variant, in which the putative degron (dotted line in **b**) was mutated to a GGS-repeat linker of the same length. Predicted protein-fragment sizes indicated. Bottom, immunoblots for YFP from transfected HeLa cells expressing either WT YFP–NS3pro-NS4A or the GGS variant, for 24 h, with or without ASV. The GGS mutation restored YFP expression in the presence of ASV. β-actin served as a loading control.

via a linker containing an NS3 protease site, can allow NS3 inhibitor application to effectively stop further protein accumulation, as is desired for our SMASh scheme (**Fig. 1a**). We thus designated the cassette comprising the NS3 protease domain, NS4A and the *cis*-cleavage site as the 'SMASh tag'.

## SMASh functions on either terminus

In the above constructs, the SMASh tag was fused to the C termini of target proteins. We next optimized the ability of the SMASh tag to remove itself from an N-terminal location. Adding linker sequences and using a faster protease cleavage site proved optimal for the drug-dependent self-removal of an N-terminal SMASh tag from the mouse Arc protein (**Supplementary Fig. 2a**). This optimized N-terminal SMASh tag regulated Arc expression with an efficacy similar to that of the C-terminal SMASh tag (**Supplementary Fig. 2b,c**). To further confirm that SMASh tags could robustly regulate proteins when present at either terminus, we coexpressed SMASh-YFP or YFP-SMASh with untagged red fluorescent protein (RFP) in HEK293 cells. In the absence of asunaprevir, YFP was liberated from either the N- or the C-terminally SMASh-tagged YFP fusions, whereas YFP protein levels were markedly reduced in the presence of the drug (**Fig. 2a**). Expression of YFP in living cells by fluorescence imaging confirmed this effect; YFP was nearly undetectable in the presence of asunaprevir (**Fig. 2b**). Treatment of the cells with drug did not affect expression of untagged RFP, thus showing the selectivity of asunaprevir for the SMASh-tagged target.

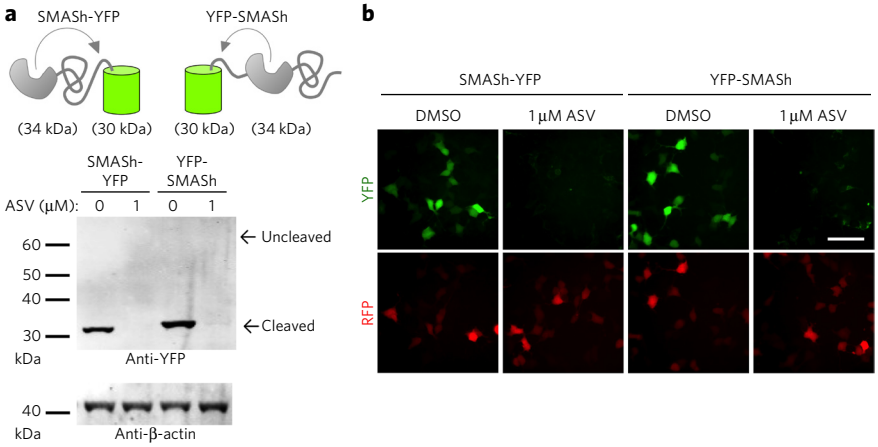


**Figure 2 | Proteins can be regulated by SMASh tags at either terminus.** (**a**) SMASh can regulate YFP when fused to either terminus. SMASh-YFP or YFP-SMASh was expressed in HEK293 cells, in the absence or presence of ASV, for 24 h. Immunoblotting revealed ASV-dependent shutoff of YFP expression from both constructs. DMSO was used as vehicle control. β-actin served as a loading control. (**b**) Fluorescence microscopy confirmed shutoff of YFP expression for both constructs after treatment with ASV. Scale bar, 50 μm.

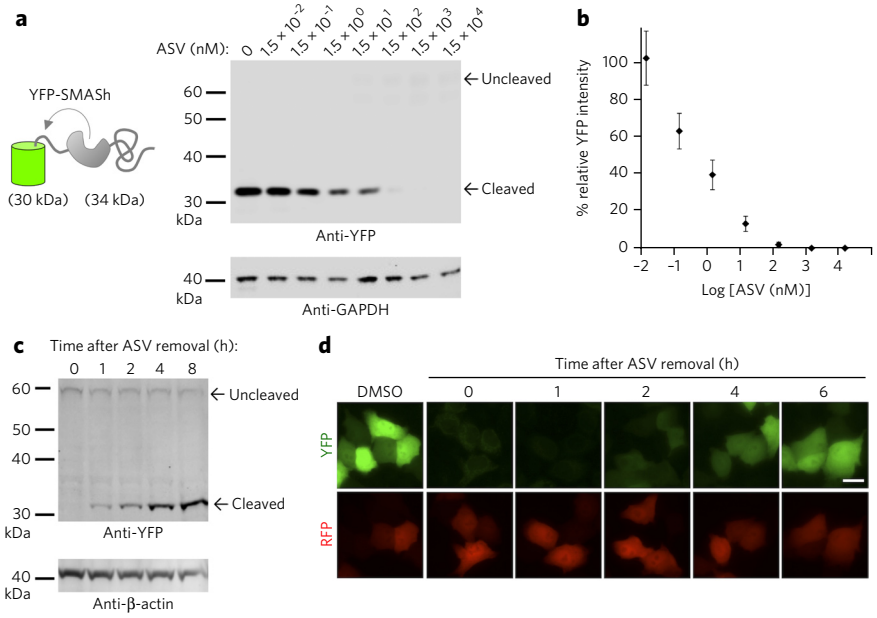


**Figure 3 | Protein regulation by SMASh-tagging is dose dependent and reversible.** (**a**) Immunoblot to detect YFP from HEK293 cells transfected with YFP-SMASh and cultured for 24 h without or with ASV (15 pM to 15 μM). GAPDH served as a loading control. (**b**) Quantification of YFP levels detected by immunoblotting. Background-subtracted YFP signal was normalized to background-subtracted GAPDH signal, and then plotted as a percentage of the signal in the untreated condition ($n$ = 3, error bars represent s.d.). (**c**) Restoration of YFP expression following drug washout, as assayed by immunoblotting. HeLa cells transfected with YFP-SMASh were grown for 12 h in the presence of 2 μM ASV, following which the cells were washed and fresh medium was applied. Parallel wells were lysed at indicated times after ASV washout. β-actin served as a loading control. (**d**) Restoration of YFP expression following drug washout, as assayed by fluorescence microscopy. HeLa cells cotransfected with untagged RFP and YFP-SMASh were grown for 12 h in the presence of 2 μM ASV, washed, resuspended in fresh medium and imaged at the indicated times after ASV washout. Transfected HeLa cells grown for 12 h in DMSO, and treated as above, are shown at left for comparison. Representative images are shown. Scale bar, 20 μm.

## Tunable, reversible and rapid control

To determine whether SMASh allows tunable control of protein levels, we treated cells expressing YFP-SMASh with asunaprevir at concentrations from 15 pM to 15 μM. YFP levels were regulated by asunaprevir in a clear dose-dependent manner (**Fig. 3a,b**). The $EC_{50}$ of asunaprevir, the effective drug concentration at which 50% of YFP expression was suppressed, was approximately 1 nM in these assays, which was comparable to its $EC_{50}$ in HCV replicon assays[11]. These results demonstrated that binding of the drug to the NS3 protease is unaltered in the SMASh-tagged construct. Notably, YFP was undetectable when cells were treated with 1.5 μM asunaprevir, a concentration at which it exhibits no activity against cellular proteases and is not cytotoxic[11]. We achieved ~98% protein repression (to protein levels 1.9% of those for undrugged cells) when cells were treated with 150 nM asunaprevir, a concentration that can be maintained in plasma and organs in humans, dogs and rodents for hours following ingestion of nontoxic doses[11,15]. Thus, SMASh-mediated repression is tunable with a >50-fold dynamic range using drug concentrations that are nontoxic and achievable *in vivo*.

Treatment with the HCV protease inhibitor prevents accumulation of new protein copies without affecting old copies, and therefore levels of the target proteins following shutoff depend on their degradation rates. Because the liberated species is no longer produced after drug addition, SMASh enables the easy measurement of protein half-lives by using

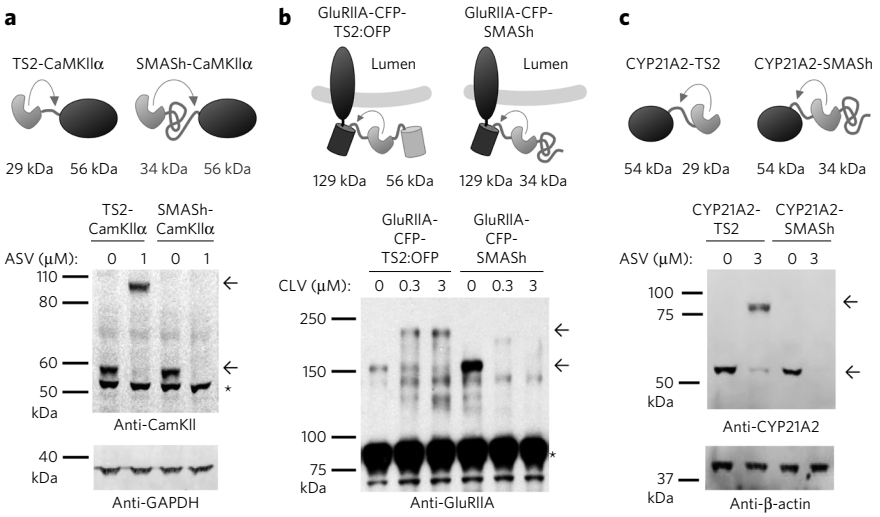


**Figure 4 | SMASh functions on a variety of proteins.** (**a**) SMASh functions on the multimerizing protein, CaMKIIα. Top, schematics of TimeSTAMP2-tagged CaMKIIα (TS2-CaMKIIα) and SMASh-CaMKIIα. Predicted protein-fragment sizes indicated. Bottom, immunoblot for CaMKIIα from HEK293 cells expressing TS2- or SMASh-CaMKIIα for 24 h in the absence or presence of ASV. The TimeSTAMP2 tag contains a *cis*-cleaving NS3 protease domain but lacks NS4A, and it was used to verify that drug inhibition of protein expression is specific to SMASh. GAPDH served as a loading control. The asterisk indicates a cross-reactive protein that was also detected in untransfected cells. The expected locations of the uncleaved higher-molecular-weight protein and the cleaved protein are indicated with arrows. (**b**) GluRIIA-CFP fused to TimeSTAMP2 with an orange fluorescent protein readout (GluRIIA-CFP-TS2:OFP) or GluRIIA-CFP-SMASh were expressed in HEK293 cells for 24 h in the absence or presence of ciluprevir (CLV). Immunoblotting revealed shutoff of GluRIIA expression by CLV. The non-degron-containing TS2:OFP tag was used to verify that CLV-dependent inhibition of protein expression is specific to SMASh. The cross-reactive bands at 80 kDa (asterisk) served as lysate loading controls. (**c**) CYP21A2 was fused to either TimeSTAMP2 or SMASh and tested by the same method as in **a**. CYP21A2 levels were detected by immunoblotting. β-actin served as a loading control.

by causing the rapid degradation of tagged proteins that are synthesized in the presence of drug. Recovery of protein expression after drug removal is rapid because mRNA pools are not depleted, which allows for the fast onset of protein production.

## Function on diverse proteins and in neurons

We next determined whether the SMASh tag can regulate production of different types of proteins. SMASh was able to control levels of a multimeric enzyme, the mouse calcium-calmodulin–activated protein kinase IIα (**Fig. 4a**), and a multipass transmembrane protein, the *Drosophila* GluRIIA glutamate receptor (**Fig. 4b**). Additionally, SMASh was able to regulate production of a short-lived protein, CYP21A2 ($t_{1/2}$ ~ 2 h, **Fig. 4c**). Thus, for the six proteins of various sizes and structures that we tested (PSD95, YFP, Arc, CaMKIIα, GluRIIA and CYP21A2), the SMASh tag conferred robust drug control.

In neurons, synthesis of specific proteins is tightly regulated by growth factors and synaptic activity and is required for long-lasting cellular changes that support memory formation. Because our previous SMASh experiments were only performed in proliferating cells, we therefore investigated whether SMASh could function in postmitotic neurons as well. We did indeed observe that the SMASh tag conferred drug-dependent control over YFP production in primary cultures of rat cortico-hippocampal and mouse cortical neurons (**Supplementary Fig. 5a**,**b**).

immunoblotting to follow decay. This principle is similar to that for the use of cycloheximide (which is often used to block all protein synthesis) in measuring protein decay rates; however, unlike cycloheximide, SMASh-mediated shutoff is specific to the tagged protein. We used SMASh to measure half-lives ($t_{1/2}$) of the relatively long-lived and short-lived proteins PSD95 ($t_{1/2}$ = 12.6 h) and human CYP21A2 ($t_{1/2}$ = 2.4 h), respectively (**Supplementary Figs. 3a** and **4a**). Next we characterized how quickly proteins with a retained SMASh tag are degraded compared to those in an untagged state. Using a simple mathematical model that relates the observed relative abundances of protein species to their rates of synthesis and degradation (see Online Methods), we found that the SMASh tag reduced the half-lives of PSD95 from 12.6 h to 1.1 h (**Supplementary Fig. 3b**) and those of CYP21A2 from 144 min to 15 min (**Supplementary Fig. 4b**).

As protease inhibitors are not known to affect mRNA transcript levels (and as evidenced by the lack of an effect of protease inhibitors on the levels of endogenous or transfected proteins not tagged by SMASh), protein shutoff by SMASh should be readily reversible upon drug removal. To test this, we incubated transiently transfected HeLa cells expressing YFP-SMASh with asunaprevir for 12 h post-transfection to ensure initial shutoff. Then, after drug washout, we followed the appearance of YFP over time. Immunoblotting showed appearance of the YFP signal within 1 h (**Fig. 3c**), whereas live-cell fluorescence microscopy showed visibility of the YFP signal within 2 h (**Fig. 3d**). The slower appearance of YFP in the fluorescence experiment is consistent with the maturation kinetics of YFP, which has a time constant of 40 min (ref. 16).

Taken together, our results demonstrate that SMASh can control protein expression in a dose-dependent and reversible manner

## SMASh functions in yeast

We next tested the efficacy of the SMASh tag in the budding yeast *Saccharomyces cerevisiae*. Yeast genes can be regulated with drug-responsive promoters, but this requires expression of an exogenous transcription factor from another gene, which abrogates endogenous transcriptional regulation[17]. Yeast protein stability can be regulated by a temperature-sensitive degron, but this induces a heat-shock response and requires switching the growth medium[18]. Among methods to control protein stability with drugs, the only one to be successfully adapted to yeast is the auxin-induced degradation (AID) method, which involves attaching proteins of interest to a domain that recruits a ubiquitin ligase in an auxin-dependent manner[18,19]. However, AID requires permanent tagging of the protein of interest and expression of a second transgene, and it can exhibit premature auxin-independent degradation or incomplete auxin-dependent degradation[18]. Thus, a method for drug-mediated regulation of protein production in yeast that is simpler and more robust is desirable.

When we expressed C-terminally SMASh-tagged YFP in yeast from an episomal gene, we found that the SMASh tag was able to suppress YFP expression in the presence of drug, as it did in mammalian cells (**Supplementary Fig. 6a**). However, the N-terminal SMASh tag, which had been optimized for efficacy in mammalian cells, showed leaky expression of YFP in the presence of drug (data not shown). Reverting the cleavage site to a slower-cleaving site (replacing EDVVPCSMG with DEMEECSQQ) fixed this problem (**Supplementary Fig. 6a**), perhaps due to HCV protease being more active at the 30 °C growth temperature for yeast than at 37 °C. SMASh was able to repress YFP expression to undetectable levels in the presence of 3 μM asunaprevir (**Supplementary**

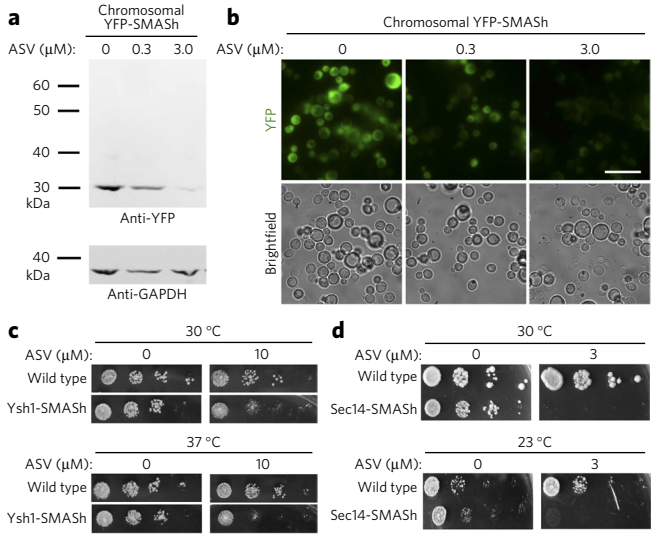


**Figure 5 | SMASh functions in *S. cerevisiae*.** (**a**) YFP-SMASh was integrated into the yeast chromosomal LUE locus under the control of the strong GPD promoter. Recombinant yeast were cultured in SD medium, in the absence or presence of ASV, for 24 h. Immunoblotting revealed shutoff of YFP expression by ASV. DMSO was used as vehicle control. GAPDH served as a loading control. (**b**) Fluorescence images of yeast cultures in **a** showing that chromosomally expressed YFP signal is controlled in a drug-dependent manner. Imaging was done in SD medium. Scale bar, 10 μm. (**c**) A SMASh tag was inserted at the C terminus of the endogenous *YSH1* coding sequence and serial dilutions of yeast cells expressing Ysh1-SMASh were plated, in the absence or presence of ASV (10 μM), and incubated for 48 h at 30 °C or 37 °C. Wild type indicates untagged strains. (**d**) An HA tag (not shown) and the SMASh tag were inserted at the C terminus of the endogenous *SEC14* coding sequence and serial dilutions of yeast cells expressing Sec14-SMASh were plated, in the absence or presence of ASV (3 μM), and incubated for 48 h at 30 °C and 23 °C.

**Fig. 6a–c**), regardless of the absence or presence of drug efflux pumps[20] (**Supplementary Fig. 6a**). These results demonstrate that SMASh confers robust drug-mediated control of protein expression in yeast (using micromolar-range drug concentrations). To the best of our knowledge, SMASh is the first method that requires only a single genetic modification to impose drug control over the expression of specific proteins in yeast.

We next determined whether SMASh could regulate the production of proteins encoded by single-copy chromosomal genes in yeast. First, we expressed YFP-SMASh from an integrated chromosomal location and again observed robust suppression of protein levels upon drug treatment (**Fig. 5a**,**b**). Next, we integrated the SMASh tag at the ends of endogenous genes encoding Ysh1, an endoribonuclease that confers a temperature-dependent growth phenotype when repressed[21], and Sec14, an essential phosphatidylinositol-phosphatidylcholine transfer protein. At 30 °C, growth of yeast cells expressing Ysh1-SMASh was normal in the absence of drug but was suppressed in the presence of drug; this effect was more pronounced at 37 °C (**Fig. 5c**). The ability of SMASh to control Ysh1 expression suggests that degradation of SMASh tags in yeast can occur at a rate considerably faster than the 30- to 45-min half-life of Ysh1 (ref. 22). Growth of Sec14-SMASh–expressing yeast was also normal in the absence of drug, but it was robustly suppressed in the presence of drug at the standard growth temperature of 30 °C (**Fig. 5d**). We also used yeast expressing Sec14-SMASh to test C-terminal SMASh-tag function at 23 °C, a temperature used by other model organisms, such as *Drosophila* or *Caenorhabditis elegans* (**Fig. 5d**). We observed that SMASh functioned at 23 °C as well. It enabled wild-type levels of growth without drug and complete growth suppression with drug, implying that both SMASh-tag cleavage and suppression of protein production are effective at 23 °C. In summary, SMASh functions in yeast to regulate the expression of episomal and chromosomal transgenes and of tagged endogenous genes, at temperatures ranging from 23 °C to 37 °C.

## SMASh enables pharmacological control over an RNA virus

Many RNA viruses infect and lyse tumor cells more efficiently than they do normal cells[23]. These viruses, which include measles virus (MeV) and vesicular stomatitis virus, are under active clinical investigation as oncolytic agents[23]. Although the agents currently being tested are nonpathogenic, safety will become a concern if these viruses are engineered for enhanced cytotoxicity or immune evasion as has been proposed[23–25], or if they are used in immunocompromised patients. It may thus be crucial to develop drug-triggered off switches. However, there are no clinically available inhibitors for most RNA viruses. Furthermore, drug-dependent transcriptional regulation is not possible with pure RNA viruses, as their life cycles bypass DNA replication and transcription. Because SMASh regulates protein production directly, we explored the possibility that it could be used as an off switch to enhance the safety of RNA virus–based therapies.

As MeV-based therapy is the most advanced in clinical testing[25], we chose to create a SMASh-controlled MeV as a model for engineering drug control into viral therapies. MeV phosphoprotein (P) brings the viral large (L) protein, an RNA-dependent RNA polymerase, to the nucleoprotein (N)-encapsidated viral genome. We hypothesized that tagging P with the SMASh tag would allow HCV protease inhibitors to block MeV replication (**Fig. 6a**). We chose to fuse the SMASh tag at the C terminus of P, as this seemed less likely to affect production of the MeV C protein, an infectivity factor whose open reading frame overlaps with that of P and begins 19 nucleotides downstream of P's start codon[26]. To inhibit viral replication, drug-mediated control of P expression needs to be rapid. We thus first performed a drug chase to determine the stability of the P protein (**Supplementary Fig. 7a**) and observed that P protein (which was produced from P-SMASh in the absence of drug) decayed noticeably after 3 h after addition of asunaprevir, indicating that P is relatively short-lived (**Supplementary Fig. 7b**). We also measured the tightness of shutoff by specifically labeling and detecting new protein copies using the methionine analog azidohomoalanine (AHA), which was added at the same time as the protease inhibitor. AHA-containing proteins were then labeled by click chemistry and purified. Immunoblotting revealed no AHA-labeled P or P-SMASh from cells incubated with AHA and asunaprevir simultaneously (**Supplementary Fig. 7b**), indicating that the inhibitor suppressed accumulation of newly synthesized P to undetectable levels. AHA-labeled P was detectable in the absence of the protease inhibitor (**Supplementary Fig. 7b**), confirming the efficacy of the labeling and purification steps. These data demonstrate that ongoing production of SMASh-tagged P protein can be robustly shut off by treatment with the protease inhibitor.

Finally, to make MeV drug controllable, we replaced the P coding region in MeV-EGFP, which also expresses enhanced green fluorescent protein (EGFP)[27], with that of P-SMASh and created MeV-EGFP-P-SMASh (**Fig. 6b** and **Supplementary Fig. 8a**). In the absence of asunaprevir, MeV-EGFP-P-SMASh replicated to titers in Vero cells similar to those for the parental MeV-EGFP (50% tissue culture infective dose ($TCID_{50}$) of $1.5 \times 10^7$/ml for MeV-EGFP-P-SMASh versus $3.8 \times 10^7$/ml for MeV-EGFP, as measured by end-point dilution, indicating the functionality of liberated P in viral replication. In the absence of drug, MeV-EGFP-P-SMASh expressed EGFP and induced syncytium formation as efficiently as did the parental MeV-EGFP (**Fig. 6c**). In contrast, in the presence of drug, whereas EGFP expression and syncytium formation by the parental MeV-EGFP remained unaffected, they were

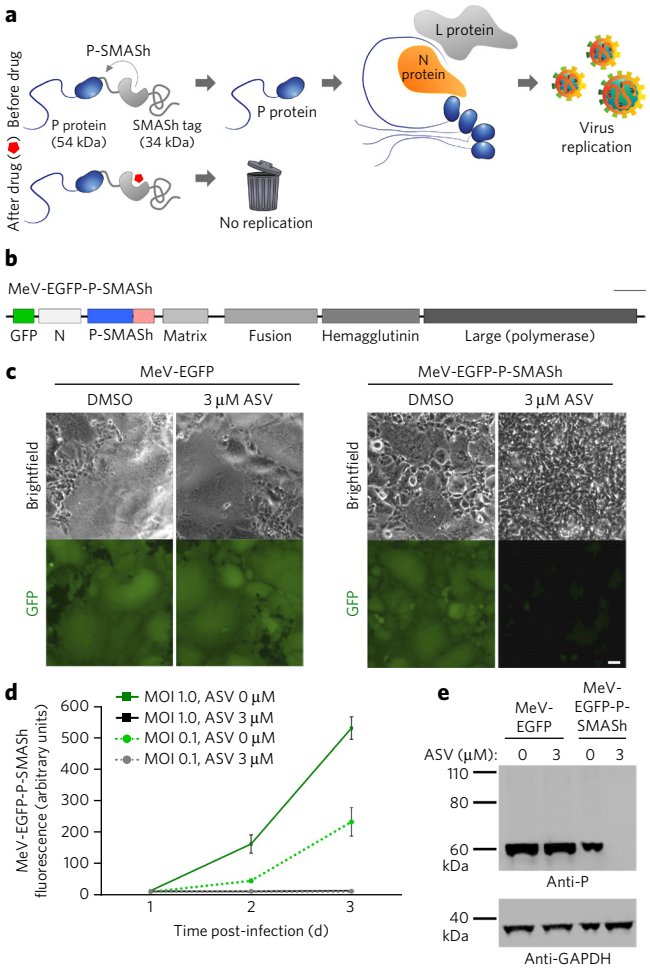


**Figure 6 | Generation of a drug-controllable 'SMAShable' measles vaccine virus.** (**a**) Concept of controlling MeV replication with P-SMASh. In the absence of the drug, unmodified phosphoprotein (P, blue) is released and can successfully form replication complexes with nucleocapsid (N, orange) and large (L) proteins. In the presence of drug, P is degraded soon after synthesis, thus preventing virus replication. (**b**) Genome organization of MeV-EGFP-P-SMASh. Scale bar, 1 kb. (**c**) Regulation of MeV-EGFP-P-SMASh by ASV. Vero cells infected with MeV-EGFP (left) or MeV-EGFP-P-SMASh (right) at a multiplicity of infection (MOI) of 1 were grown for 72 h in the absence or presence of ASV. Drug inhibited syncytium formation (brightfield, top) and GFP expression (GFP, bottom) in MeV-EGFP-P-SMASh-infected, but not in MeV-EGFP-infected, cells. Scale bar, 50 μm (all panels are at the same scale). (**d**) Quantification of fluorescence from Vero cells infected with MeV-EGFP-P-SMASh at MOI of 1 and 0.1, in the absence or presence of 3 μM ASV ($n$ = 3, error bars are s.d.). (**e**) Drug inhibited P expression in cells infected with MeV-EGFP-P-SMASh, but not in those infected with MeV-EGFP, as assayed by immunoblotting. GAPDH served as a loading control.

completely abolished for cells infected with MeV-EGFP-P-SMASh (**Fig. 6c**). Suppression was remarkably effective, with drug suppressing 97.3% of EGFP fluorescence 3 d post-transfection when compared to that for the untreated case (**Fig. 6d** and **Supplementary Fig. 8b**). Immunoblotting confirmed that asunaprevir treatment efficiently inhibited P production in virus-infected cells (**Fig. 6e**). Thus, in summary, SMASh allowed us to render MeV exquisitely sensitive to inhibition by HCV NS3 protease inhibitors. Through the simple insertion of a SMASh tag in one viral gene, we were able to create a drug-regulatable version of this RNA virus for which no specific clinically approved inhibitors previously existed.

## DISCUSSION

We have presented a new approach, SMASh, for the drug-mediated regulation of protein production. SMASh is unique in combining multiple desirable features, including rapid onset, reversible and robust drug regulation of protein expression, the requirement for only a single genetic modification, minimal modification to proteins of interest and use of a clinically approved drug. SMASh satisfies a longstanding need for a simple, generalizable method for reversible drug-dependent control of protein production, while allowing protein expression with minimal perturbation[28].

Earlier strategies to control specific protein levels via drug-dependent degradation or stabilization either substantially change target protein structure or require multiple components (**Supplementary Table 1**). Domains that are unstable in the absence[29–31] or presence[32,33] of drug binding allow chemical control of protein abundance and, like SMASh, function autonomously as single genetic tags. However, unlike SMASh, these fusions are permanent. The AID system of drug-induced destabilization requires both the attachment of a large domain and coexpression of a second protein[18]. Because fusion of smaller peptides preserves protein function in some cases where larger domains such as GFP do not[34], SMASh should be less likely to perturb target protein function than methods that involve the permanent attachment of large domains. For example, both termini of the MeV P protein are believed to interact with N protein[35,36], and P-GFP and GFP-P fusions block and severely hinder MeV replication[37], respectively. By contrast, MeV expressing P-SMASh replicated similarly to parental virus. Minimal protein modification may also be useful in yeast, as a large percentage of yeast proteins may be adversely affected by the attachment of long protein sequences. For instance, among 2,086 yeast proteins whose localization was studied by fusion to a 237-residue GFP tag or a 93-residue tag containing multiple hemagglutinin (HA) epitopes, a large proportion (32%) showed different patterns of localization with the two tags, suggesting that at least one of the tags causes protein mislocalization[38].

Earlier methods to control the production of untagged proteins using established drugs also have limitations in complexity, performance or generalizability. In the 'split ubiquitin for the rescue of function' (SURF) method, drug-induced ubiquitin fragment complementation triggers degron removal from the C terminus of a protein of interest, which can be traceless if the native C terminus is accessible to ubiquitin hydrolases[39]. However, SURF involves expression of a target-protein fusion plus expression of a complementation partner and is leaky unless components are further regulated by drug-inducible transcription, which then necessitates expression of the drug-regulated transcription factor as a third protein and the use of a second drug[40]. Ubiquitin ligases have been fused to protein-binding domains that enable recognition of specific targets, including unmodified endogenous proteins[41], with temporal regulation being supplied by drug-inducible transcription. This approach thus also requires two components, the fusion protein and a drug-regulated transcription factor, and its implementation depends on the availability of targeting domains for proteins of interest. Notably, the nature of chemical regulation in this system is purely transcriptional. As SMASh-mediated control is faster than transcriptional regulation, it can be used in place of drug-regulated transcription to improve the performance of the above methods. However, it may be easier to simply tag the protein of interest directly with a SMASh tag and obviate the need for other genetic modifications. Indeed, recently developed genome-editing technologies may enable the tagging of endogenous genes with SMASh tags in various cell types.

Finally, one method, Protacs, does not require expression of any artificial proteins at all, as it uses bivalent small molecules to bring ubiquitin ligases to protein targets[42]. However, in Protacs, small molecules must be developed for each protein target if they do not exist already. The generation of small molecules that are nontoxic in

cells and animals and specific for a protein target is not assured for a given protein. Each new case would require an extensive drug development effort, rendering this approach not easily generalizable.

Indeed, a notable feature of SMASh is that it uses HCV protease inhibitors, which are already approved for long-term use in humans. SMASh uses drug concentrations that are achievable *in vivo* in mammals without toxicity, in contrast to some other techniques[33,43]. Our experiments also indicate that asunaprevir is able to efficiently cross the yeast cell wall. Even when transcribed from episomes using the strong glyceraldehyde-3-phosphate dehydrogenase (GPD) promoter, levels of SMASh-tagged YFP protein were effectively suppressed by 3 μM asunaprevir. In contrast, 1,000 μM auxin was required for AID to suppress production of a protein expressed from the ten-fold weaker alcohol dehydrogenase 1 (ADH1) promoter[18,44].

SMASh differs from most other strategies for regulating protein stability in that it selectively controls the degradation of new copies of a protein of interest, and not preexisting copies. Cells respond rapidly to environmental stimuli such as growth signals[45] or, in the nervous system, synaptic activity[7] by synthesizing new proteins. SMASh can be used to query the roles of specific new protein species in such biological responses. SMASh can also be used to estimate half-lives of proteins of interest, as the persistence of untagged protein copies that were produced in the absence of drug can be measured over time, while accumulation of newly synthesized target-protein molecules is inhibited in the presence of drug. Here, SMASh can be used similarly to cycloheximide or anisomycin to estimate protein half-lives[46], but with much less toxicity. By inhibiting all protein synthesis in the cell, cycloheximide and anisomycin can be expected to impair cell health and to generate erroneous half-life calculations as the levels of proteins that regulate the stability of the protein of interest also drop. The SMASh system may thus be especially advantageous for measuring half-lives of long-lived proteins such as PSD95 (**Supplementary Fig. 3a**).

SMASh also allows rapid increases in protein levels. Expression of a protein can be repressed with drug; then, when expression is desired, the drug can be washed out. Protein molecules will then immediately begin to accumulate as a result of the ongoing translation of existing mRNAs. Upregulating protein levels by reversing SMASh shutoff should be faster than by inducing gene transcription, which takes many hours in mammalian systems[47].

RNA viruses that replicate more efficiently in certain neoplastic cell types have long been considered as targeted cancer treatments. However, only viruses that are nonpathogenic or cause mild disease, such as vaccine-strain MeV, are currently being tested in clinical trials. As the self-limiting nature of these viruses will likely limit their oncolytic efficacy, researchers have proposed modifying them to increase cytotoxicity or immune evasion[48,49]. Such steps could lead to unexpected side effects[50], and it would be desirable to have pharmacological methods for terminating the replication of engineered viruses[24]. We found that SMASh enabled robust control of MeV, for which no clinically available specific inhibitors exist, by HCV NS3 protease inhibitors. We expect that other viruses can be controlled by SMASh tagging as well.

In summary, SMASh has advantages over other methods of controlling the levels of proteins of interest in that it minimizes protein modification, requires only one genetically encoded modification and uses clinically available drugs that are nontoxic and cell permeable. Furthermore, SMASh functions robustly in mitotic and nonmitotic mammalian cells and in yeast. Using SMASh, we have also engineered, for the first time, an RNA virus that can be tightly regulated by a drug without the need to develop new, virus-specific small-molecule inhibitors. Thus, with its ease of implementation and generalizability, the SMASh technique can be applied to a variety of problems in biomedicine and biotechnology, ranging from the study of gene function to the engineering of drug-dependent features in cellular and viral therapies.

Received 11 September 2014; accepted 10 June 2015; published online 27 July 2015

## METHODS

Methods and any associated references are available in the online version of the paper.

## References


1. Sigoillot, F.D. & King, R.W. Vigilance and validation: keys to success in RNAi screening. *ACS Chem. Biol.* **6**, 47–60 (2011).
2. Vogel, C. & Marcotte, E.M. Insights into the regulation of protein abundance from proteomic and transcriptomic analyses. *Nat. Rev. Genet.* **13**, 227–232 (2012).
3. Wu, L. *et al.* Variation and genetic control of protein abundance in humans. *Nature* **499**, 79–82 (2013).
4. Battle, A. *et al.* Genomic variation. Impact of regulatory variation from RNA to protein. *Science* **347**, 664–667 (2015).
5. Huang, C.J. *et al.* Conditional expression of a myocardium-specific transgene in zebrafish transgenic lines. *Dev. Dyn.* **233**, 1294–1303 (2005).
6. Matsukura, S., Jones, P.A. & Takai, D. Establishment of conditional vectors for hairpin siRNA knockdowns. *Nucleic Acids Res.* **31**, e77 (2003).
7. Butko, M.T. *et al.* Fluorescent and photo-oxidizing TimeSTAMP tags track protein fates in light and electron microscopy. *Nat. Neurosci.* **15**, 1742–1751 (2012).
8. Lin, M.Z., Glenn, J.S. & Tsien, R.Y. A drug-controllable tag for visualizing newly synthesized proteins in cells and whole animals. *Proc. Natl. Acad. Sci. USA* **105**, 7744–7749 (2008).
9. Jiang, Y. *et al.* Discovery of danoprevir (ITMN-191/R7227), a highly selective and potent inhibitor of hepatitis C virus (HCV) NS3/4A protease. *J. Med. Chem.* **57**, 1753–1769 (2014).
10. Lamarre, D. *et al.* An NS3 protease inhibitor with antiviral effects in humans infected with hepatitis C virus. *Nature* **426**, 186–189 (2003).
11. McPhee, F. *et al.* Preclinical profile and characterization of the hepatitis C virus NS3 protease inhibitor asunaprevir (BMS-650032). *Antimicrob. Agents Chemother.* **56**, 5387–5396 (2012).
12. Talwani, R., Heil, E.L., Gilliam, B.L. & Temesgen, Z. Simeprevir: a macrocyclic HCV protease inhibitor. *Drugs Today (Barc)* **49**, 769–779 (2013).
13. Brass, V. *et al.* Structural determinants for membrane association and dynamic organization of the hepatitis C virus NS3–4A complex. *Proc. Natl. Acad. Sci. USA* **105**, 14545–14550 (2008).
14. Yao, N., Reichert, P., Taremi, S.S., Prosise, W.W. & Weber, P.C. Molecular views of viral polyprotein processing revealed by the crystal structure of the hepatitis C virus bifunctional protease-helicase. *Structure* **7**, 1353–1363 (1999).
15. Yuan, L. *et al.* A rugged and accurate liquid chromatography–tandem mass spectrometry method for the determination of asunaprevir, an NS3 protease inhibitor, in plasma. *J. Chromatogr. B Analyt. Technol. Biomed. Life Sci.* **921–922**, 81–86 (2013).
16. Iizuka, R., Yamagishi-Shirasaki, M. & Funatsu, T. Kinetic study of *de novo* chromophore maturation of fluorescent proteins. *Anal. Biochem.* **414**, 173–178 (2011).
17. Mnaimneh, S. *et al.* Exploration of essential gene functions via titratable promoter alleles. *Cell* **118**, 31–44 (2004).
18. Morawska, M. & Ulrich, H.D. An expanded tool kit for the auxin-inducible degron system in budding yeast. *Yeast* **30**, 341–351 (2013).
19. Nishimura, K., Fukagawa, T., Takisawa, H., Kakimoto, T. & Kanemaki, M. An auxin-based degron system for the rapid depletion of proteins in nonplant cells. *Nat. Methods* **6**, 917–922 (2009).
20. Su, L.J. *et al.* Compounds from an unbiased chemical screen reverse both ER-to-Golgi trafficking defects and mitochondrial dysfunction in Parkinson's disease models. *Dis. Model. Mech.* **3**, 194–208 (2010).
21. Garas, M., Dichtl, B. & Keller, W. The role of the putative 3′ end processing endonuclease Ysh1p in mRNA and snoRNA synthesis. *RNA* **14**, 2671–2684 (2008).
22. Belle, A., Tanay, A., Bitincka, L., Shamir, R. & O'Shea, E.K. Quantification of protein half-lives in the budding yeast proteome. *Proc. Natl. Acad. Sci. USA* **103**, 13004–13009 (2006).
23. Miest, T.S. & Cattaneo, R. New viruses for cancer therapy: meeting clinical needs. *Nat. Rev. Microbiol.* **12**, 23–34 (2014).
24. Russell, S.J., Peng, K.W. & Bell, J.C. Oncolytic virotherapy. *Nat. Biotechnol.* **30**, 658–670 (2012).
25. Msaouel, P., Opyrchal, M., Domingo Musibay, E. & Galanis, E. Oncolytic measles virus strains as novel anticancer agents. *Expert Opin. Biol. Ther.* **13**, 483–502 (2013).
26. Rima, B.K. & Duprex, W.P. The measles virus replication cycle. *Curr. Top. Microbiol. Immunol.* **329**, 77–102 (2009).
27. Zuniga, A. *et al.* Attenuated measles virus as a vaccine vector. *Vaccine* **25**, 2974–2983 (2007).

28. Lampson, M.A. & Kapoor, T.M. Targeting protein stability with a small molecule. *Cell* **126**, 827–829 (2006).
29. Banaszynski, L.A., Chen, L.-C., Maynard-Smith, L.A., Ooi, A.G.L. & Wandless, T.J. A rapid, reversible and tunable method to regulate protein function in living cells using synthetic small molecules. *Cell* **126**, 995–1004 (2006).
30. Iwamoto, M., Bjorklund, T., Lundberg, C., Kirik, D. & Wandless, T.J. A generalchemical method to regulate protein stability in the mammalian central nervous system. *Chem. Biol.* **17**, 981–988 (2010).
31. Stankunas, K. *et al.* Conditional protein alleles using knock-in mice and a chemical inducer of dimerization. *Mol. Cell* **12**, 1615–1624 (2003).
32. Bonger, K.M., Chen, L.C., Liu, C.W. & Wandless, T.J. Small-molecule displacement of a cryptic degron causes conditional protein degradation. *Nat. Chem. Biol.* **7**, 531–537 (2011).
33. Tae, H.S. *et al.* Identification of hydrophobic tags for the degradation of stabilized proteins. *ChemBioChem* **13**, 538–541 (2012).
34. Andresen, M., Schmitz-Salue, R. & Jakobs, S. Short tetracysteine tags to β-tubulin demonstrate the significance of small labels for live cell imaging. *Mol. Biol. Cell* **15**, 5616–5622 (2004).
35. Chen, M., Cortay, J.C. & Gerlier, D. Measles virus protein interactions in yeast: new findings and caveats. *Virus Res.* **98**, 123–129 (2003).
36. Shu, Y. *et al.* Plasticity in structural and functional interactions between the phosphoprotein and nucleoprotein of measles virus. *J. Biol. Chem.* **287**, 11951–11967 (2012).
37. Devaux, P. & Cattaneo, R. Measles virus phosphoprotein gene products: conformational flexibility of the P/V protein amino-terminal domain and C protein infectivity factor function. *J. Virol.* **78**, 11632–11640 (2004).
38. Huh, W.K. *et al.* Global analysis of protein localization in budding yeast. *Nature* **425**, 686–691 (2003).
39. Pratt, M.R., Schwartz, E.C. & Muir, T.W. Small-molecule–mediated rescue of protein function by an inducible proteolytic shunt. *Proc. Natl. Acad. Sci. USA* **104**, 11209–11214 (2007).
40. Lin, Y.H. & Pratt, M.R. A dual small-molecule rheostat for precise control of protein concentration in mammalian cells. *ChemBioChem* **15**, 805–809 (2014).
41. Cong, F., Zhang, J., Pao, W., Zhou, P. & Varmus, H. A protein knockdown strategy to study the function of β-catenin in tumorigenesis. *BMC Mol. Biol.* **4**, 10 (2003).
42. Sakamoto, K.M. *et al.* Protacs: chimeric molecules that target proteins to the Skp1–Cullin–F box complex for ubiquitination and degradation. *Proc. Natl. Acad. Sci. USA* **98**, 8554–8559 (2001).
43. Limenitakis, J. & Soldati-Favre, D. Functional genetics in Apicomplexa: potentials and limits. *FEBS Lett.* **585**, 1579–1588 (2011).
44. Mumberg, D., Muller, R. & Funk, M. Yeast vectors for the controlled expression of heterologous proteins in different genetic backgrounds. *Gene* **156**, 119–122 (1995).
45. Shimobayashi, M. & Hall, M.N. Making new contacts: the mTOR network in metabolism and signaling crosstalk. *Nat. Rev. Mol. Cell Biol.* **15**, 155–162 (2014).
46. Zhou, P. Determining protein half-lives. *Methods Mol. Biol.* **284**, 67–77 (2004).
47. Shoulders, M.D., Ryno, L.M., Cooley, C.B., Kelly, J.W. & Wiseman, R.L. Broadly applicable methodology for the rapid and dosable small molecule–mediated regulation of transcription factors in human cells. *J. Am. Chem. Soc.* **135**, 8129–8132 (2013).
48. Cattaneo, R., Miest, T., Shashkova, E.V. & Barry, M.A. Reprogrammed viruses as cancer therapeutics: targeted, armed and shielded. *Nat. Rev. Microbiol.* **6**, 529–540 (2008).
49. Meng, X. *et al.* Enhanced antitumor effects of an engineered measles virus Edmonston strain expressing the wild-type N, P, L genes on human renal cell carcinoma. *Mol. Ther.* **18**, 544–551 (2010).
50. Chen, N. *et al.* Poxvirus interleukin-4 expression overcomes inherent resistance and vaccine-induced immunity: pathogenesis, prophylaxis and antiviral therapy. *Virology* **409**, 328–337 (2011).


## Acknowledgments

We thank M. Billeter (University of Zurich) for p(+)-MeV plasmid, Y. Yanagi (Kyushu University) for Vero-hSLAM cells, M. Takeda (Kyushu University) for the MeV IC-B strain, J. Glenn (Stanford University) for BILN-2061, and A. Gitler, T. Stearns, A. Morrison and J. Skotheim (Stanford University) for yeast plasmids and reagents. We also thank Y. Geng of the Lin laboratory for performing brain dissections, other members of the Lin laboratory for advice, S. Beckwith of the Morrison laboratory for training on yeast procedures and A. Gitler and G. Sherlock (Stanford University) for critical reading of the manuscript. This work was supported by Stanford Graduate Fellowships (H.K.C. and C.L.J.); a US National Science Foundation Graduate Research Fellowship (C.L.J.); NIAID, US National Institutes of Health (NIH) grants 5R01AI071002 and 5R01AI083402 (R.K.P.); NIGMS, NIH EUREKA grant 5R01GM098734 (M.Z.L.); a Burroughs Wellcome Foundation Career Award for Medical Scientists (M.Z.L.); and an Alliance for Cancer Gene Therapy Young Investigator Award (M.Z.L.).

## Author contributions

H.K.C. optimized SMASh, performed mammalian cell, yeast and virus experiments, and wrote the manuscript. C.L.J. performed mammalian cell experiments and contributed to the manuscript. J.Y. optimized SMASh and performed mammalian cell experiments. Y.H. performed mammalian cell experiments. S.A.K. packaged virus. R.K.P. packaged virus and provided advice. R.Y.T. provided advice. M.Z.L. designed SMASh, performed mammalian cell experiments, directed the project and wrote the manuscript.

## Competing financial interests

The authors declare no competing financial interests.

## Additional information

Supplementary information is available in the online version of the paper. Reprints and permissions information is available online at http://www.nature.com/reprints/index.html. Correspondence and requests for materials should be addressed to M.Z.L.

## ONLINE METHODS

**DNA constructs.** Plasmids encoding PSD95 or Arc fused to TimeSTAMP cassettes[17,18] were modified by standard molecular biology techniques including PCR, restriction enzyme digestion and ligation or In-Fusion enzyme (Clontech) to create new TimeSTAMP variants or SMASh variants. All subcloned fragments were sequenced in their entirety to confirm successful construction. Full sequences of all plasmids used in this study are available upon request.

**Cell culture and transfection.** Authenticated HEK293 (Life Technologies) and Vero (American Type Culture Collection) cells were directly purchased from the vendor. HeLa cells (kind gift from M. Kay (Stanford University)) were morphologically correct. All cells were determined to be negative for mycoplasma using the MycoAlert detection kit (Lonza). HEK293, Vero and HeLa cell lines were cultured at 37 °C in 5% $CO_2$ in Dulbecco's modified Eagle's medium (DMEM, HyClone) supplemented with 10% FBS (Gibco), 2 mM glutamine (Life Technologies) and 100 U/mL penicillin and 100 µg/mL streptomycin (Life Technologies). Cells were transfected using Lipofectamine 2000 (Life Technologies) in Opti-MEM (Life Technologies) according to the manufacturer's recommended protocol.

**Chemical reagents.** HCV NS3 inhibitors ciluprevir (CLV) and asunaprevir (ASV) were obtained by custom synthesis (Acme Bioscience) and dissolved in DMSO (Thermo Scientific) at 3 mM for medium-term storage at −20 °C. These were then diluted into media to achieve the desired final concentrations (1–3 µM) for treatment of cells. Further serial dilutions were performed for the dose-dependency experiment. For long-term CLV and ASV incubations, drug was applied either simultaneously with transfection media or 1–2 h after transfection. MG132 (Sigma) was dissolved in DMSO for a 1000× working stock of 10 mM. Bortezomib (Adooq Biosciences) was dissolved in DMSO for a 500× working stock of 33 µM. Chloroquine diphosphate salt (Sigma) was dissolved in $H_2O$ for a 1,000× (100 mM) working stock. Bafilomycin A1 (Santa Cruz) was dissolved in DMSO for a 500× (100 µM) working stock. Azidohomoalanine (AHA) (Click-IT, Invitrogen) was dissolved in DMSO for a 500× working stock of 25 mM. Alkyne-PEG4-biotin (Invitrogen) was dissolved in DMSO for a 100× working stock of 4 mM. L-cystine dihydrochloride (Sigma) was dissolved in $H_2O$ pH 2.0 for a working stock of 0.1 M.

**Yeast strains and cell growth.** All experiments were carried out in the W303-1A *ADE2*$^+$ strain background[51] and a pump-deficient W303-1A strain (*MATa can1-100 his3-11,15 leu2-3,112 trp1-1 ura3-1 ade2-1 pdr1*::kanMX *pdr3*::kanMX)[20]. SMASh strains were made by transformation of yeast episomal plasmid (pAG426) or yeast integrating plasmid (pRS405), expressing SMASh-fused YFP under GPD promoter. Yeastmaker DNA kit (Clontech) was used for yeast lithium acetate–mediated yeast transformations. Cells were grown at 30 °C in SD (synthetic-defined) medium or YPD (yeast extract–peptone–dextrose) medium. To generate SMASh knock-in yeast, PCR fragments containing the SMASh tag followed by the yeast ADH1 terminator and NatMX (clonNAT resistance gene) were inserted before the termination codon of the protein of interest by homologous recombination. To perform yeast spotting assay, YPD plates were prepared with ASV or the same concentration of DMSO (1% v/v).

**Primary neuronal culture.** All animal procedures were approved by the Stanford University Administrative Panel on Laboratory Animal Care and were performed in accordance with the applicable regulatory standards. Sprague-Dawley rat E15 cortico-hippocampal tissue and FVB mouse E18 cortical tissue were dissected, incubated in RPMI (Life Technologies) with papain (Worthington) and DNase I (Roche) for dissociation, triturated and electroporated using the Amaxa rat or mouse Neuron Nucleofector Kit (Lonza), before being plated on poly-L-lysine–coated four-chamber 35-mm glass-bottom dishes (*In vitro* Scientific), in the presence of 5–10% FBS (Gibco), at a density of ~150,000 neurons per quadrant. Neurons were cultured in NeuroBasal medium (Life Technologies) supplemented with GlutaMAX, B-27 and penicillin-streptomycin (pen-strep) solution (Life Technologies) at 37 °C with 5% $CO_2$. Every 3 d, 50% of media was refreshed.

**Virus cloning, packaging and infection.** To construct p(+)-MeV-EGFP-PSMASh, DNA encoding the SMASh tag was added in frame to the P open reading frame in p(+)-MeV-EGFP; the resulting full-length clone was corrected for the paramyxovirus rule-of-six and verified through sequencing. Recombinant MeV were recovered using a modified rescue system[52]. BSR–T7-5 cells[53] were transfected with p(+)-MeV-EGFP or p(+)-MeV-EGFP-PSMASh, respectively, and plasmids encoding the L, N or P proteins, which were derived from the MeV IC-B strain[54]. All constructs were under the control of the T7 promoter. 48 h post-transfection, BSR–T7-5 helper cells were overlaid on Vero cells, which were stably expressing human CD150 and SLAM[55], and the overlay plates were incubated at 32 °C until infectious centers became detectable. Virions from individual centers were transferred to fresh Vero-SLAM cells for generation of passage-two virus stocks. To confirm integrity of recombinant viruses, RNA was extracted from infected cells using the RNeasy mini kit (Qiagen) and cDNAs were created using random hexamer primers and Superscript III reverse transcriptase (Life Technologies). PCR was performed with primers 28-F: TAATCTCCAAGCTAGAATC and 35-R: AGCCTGCCATCACTGTA (**Supplementary Fig. 9**) and sequenced. To prepare virus stocks, Vero cells were infected at a multiplicity of infection (MOI) of 0.01 $TCID_{50}$/cell with the relevant virus and incubated at 32 °C until cytopathic effect (CPE) became detectable. Plates were then moved to 37 °C and incubated until there was 100% CPE. Cells were scraped in Opti-MEM (Life Technologies) and particles released by two freeze-thaw cycles. Titers were determined by $TCID_{50}$ titration on Vero cells according to the Spearman-Karber method as described[56]. Virus infection for drug controllability tests was initiated through inoculation of Vero cells at an MOI of 0.1 and 1 $TCID_{50}$/cell at 32 °C.

**Microscopy.** For imaging of MeV-infected cells, brightfield and fluorescence microscopy were performed on a Nikon TE300 microscope with a 10× 0.25-numerical aperture (NA) objective. HEK293A cells were imaged with a 20× 0.15 NA objective on the same microscope. The cells were cultured in 12-well plates (Greiner), and MeV-infected cells were imaged in culture media (10% FBS supplemented phenol red free DMEM), whereas HEK293 cells were imaged in HBSS. Brightfield and fluorescence microscopy of yeast were done with an Olympus 100× 1.4-NA oil-immersion objective on Olympus IX80 microscope. Yeast cells were imaged in SD medium in a concanavalin A (ConA)-coated (Sigma) TC CU109 chamber (Chamlide). For HeLa cells and neurons, microscopy was performed on a Zeiss Axiovert 200M with a 40× 1.2-NA water immersion objective. These cells were cultured in four-chamber, 35-mm glass bottom dishes (*In vitro* Scientific) and culture media were replaced with HBSS during live-imaging sessions. All microscopes were connected to Hamamatsu ORCA-ER cameras and controlled by Micro-Manager software. Image processing was performed in ImageJ.

**Immunoblotting.** After washing twice with PBS, cells were lysed with 50–100 µl of hot SDS lysis buffer (100 mM Tris HCl pH 8.0, 4% SDS, 20% glycerol, 0.2% bromophenol blue, 10% 2-mercaptoethanol) and DNA was sheared by sonication. After heating to 80–90 °C for several minutes, cell lysates along with Novex Sharp prestained protein standard (Life Technologies) or Precision Plus Protein Dual Color Standards (Bio-Rad) were loaded onto 4–12% Bis-Tris gels (NuPAGE, Life Technologies), dry-transferred to nitrocellulose or PVDF membranes (iBlot system, Life Technologies), probed with primary and secondary antibodies, and imaged using LI-COR Odyssey imaging system. Quantification of immunoblots was performed in ImageJ.

**Antibodies.** The following primary antibodies were used for immunoblotting at the indicated dilutions: mouse monoclonal anti-PSD95 (NeuroMab, clone K28-43), 1:2,000; mouse monoclonal anti-Arc (Santa Cruz, clone C7, sc-17839), 1:200; mouse monoclonal anti-GFP (Pierce, clone GF28R, MA5-15256), 1:1,000; rabbit monoclonal anti-GFP (Abcam, clone E385, ab32146), 1:1,000; rabbit polyclonal anti-β-actin (GeneTex, GTX124214) 1:10,000; mouse monoclonal anti-GAPDH (Santa Cruz, clone G-9, sc-365062), 1:4,000; rabbit polyclonal anti-GAPDH (Santa Cruz, sc-25778), 1:4,000; mouse monoclonal anti-GAPDH (Pierce, clone GA1R, MA5-15738), 1:1,000; mouse monoclonal anti–measles phosphoprotein (P) (Novus, clone 9H4, NB110-37247 or Abcam, clone 9H4, ab43820), 1:200; rabbit polyclonal anti-CamKIIα (Santa Cruz, sc-13082), 1:200; mouse monoclonal anti-GluRIIA (DSHB, 8B4D2), 1:1,000; anti-CYP21A2 (Santa Cruz, clone C-17, sc-48466), 1:200; and rabbit monoclonal anti-HA (Cell Signaling, C29F4), 1:1,000. Secondary antibodies were LI-COR 680RD goat–anti-mouse, 680RD goat–anti-rabbit, 800CW goat–anti-mouse or 800CW goat–anti-rabbit antibodies; all used at 1:5,000.

**Metabolic labeling, click chemistry and pulldown.** HeLa cells were cultured in 12-well plates (Greiner) in standard DMEM supplemented with glutamine,

pen-strep and 10% FBS. 20 h after transfection, wells were washed 3× with HBSS, and cells were methionine-depleted via 30-min incubation in metabolic-label DMEM (methionine-cystine–free DMEM (Corning Cellgro) supplemented with glutamine, pen-strep, 0.2 mM L-cystine (Sigma) and 10% dialyzed FBS (Thermo)). Following the depletion step, medium was replaced with either standard DMEM, metabolic-label DMEM with 50 μM AHA, or metabolic-label DMEM with 50 μM AHA and 2 μM ASV. Equivalent volumes of DMSO were used in '0 μM ASV' wells. Incubation for labeling lasted 3 h, after which each well was washed and cells lysed with 50 μL gentle lysis buffer (1% SDS, 50 mM Tris HCl pH 8.0, EDTA-free protease inhibitor cocktail (Complete Mini, Roche), phosphatase inhibitor cocktail (Halt, Pierce), 3 μM ASV). For each condition, lysates from three separate wells were pooled. Lysates were sonicated and clarified by centrifugation. For pre-click–pulldown samples, 50 μL of each lysate was reserved and combined with 50 μL of hot SDS lysis buffer for SDS-PAGE analysis.

For click reactions, 50 μL of each lysate was processed using the Click-IT Protein Reaction Buffer kit (Invitrogen) with alkyne-PEG4-biotin (Invitrogen) according to the manufacturer's recommendations. Following click labeling, methanol-chloroform–extracted protein pellets were resuspended by vortexing in 20 μL of gentle lysis buffer + 80 μL of nondenaturing buffer (1% Nonidet P40, 50 mM Tris HCl pH 8.0, EDTA-free protease inhibitor cocktail). Proteins were allowed to solubilize at 4 °C overnight. Biotin-labeled proteins were purified via a magnetic streptavidin bead (PureProteome, Millipore) pulldown. Prior to setting up the binding reactions, beads were blocked by incubating with 5% BSA solution in PBS for 1 h on a rotator at room temp, and washing 3× in PBS-T (PBS plus 0.1% Tween-20). Beads were resuspended in PBS-T. Binding reactions (200 μL volume) proceeded for 1 h on a rotator at room temp, after which the beads were washed 3× with PBS-T. Proteins were eluted for SDS-PAGE by heating beads in 50 μL SDS lysis buffer at 95 °C for 10 min.

**Calculating half-lives of SMASh-tagged proteins.** To calculate production rates of PSD95 and PSD95-SMASh, we assumed that the protein production rates were constant between 24 and 28 h post-transfection and were the same for the PSD95-SMASh protein expressed from a PSD95-SMASh gene (in the presence of ASV) and the PSD95 protein expressed from a PSD95-SMASh gene (in the absence of ASV). The rate of change in protein concentrations can be modeled with the differential equations

$$d[\mathrm{PSD95}]_{(t)}/dt = k_{\mathrm{syn,PSD}} - k_{\mathrm{deg,PSD95}}[\mathrm{PSD95}]_{(t)} \quad (1)$$

$$d[\mathrm{PSD95SMASh}]_{(t)}/dt = k_{\mathrm{syn,PSDSMASh}} - k_{\mathrm{deg,PSD95SMASh}}[\mathrm{PSD95SMASh}]_{(t)} \quad (2)$$

where $[\mathrm{PSD95}]_{(t)}$ is protein concentration of PSD95 at time t, $[\mathrm{PSD95SMASh}]_{(t)}$ is protein concentration of PSD95-SMASh at time t, $k_{\mathrm{syn,PSD95}}$ and $k_{\mathrm{syn,PSD95SMASh}}$ are production rate constants of PSD95 and PSD95-SMASh, respectively, and $k_{\mathrm{deg,\ PSD95}}$ and $k_{\mathrm{deg,\ PSD95SMASh}}$ are decay rate constants of PSD95 and PSD95-SMASh, respectively. Integration of these equations yields

$$[\mathrm{PSD95}]_{(t)} = (k_{\mathrm{syn,PSD}}/k_{\mathrm{deg,PSD95}})(1 - e^{-k\,\mathrm{deg,PSD95}t}) \quad (3)$$

$$[\mathrm{PSD95SMASh}]_{(t)} = (k_{\mathrm{syn,PSD95SMASh}}/k_{\mathrm{deg,PSD95SMASh}})(1 - e^{-k\,\mathrm{deg,PSD95SMASh}t}) \quad (4)$$

We measured PSD95 half-life ($t_{1/2,\ \mathrm{PSD95}}$) by fitting the PSD95 band intensities of different time points to monoexponential decay curves ($n = 3$), and obtained 12.6 h. We then determined the decay rate constant of PSD95 ($k_{\mathrm{deg,\ PSD95}} = \ln_2/t_{1/2,\ \mathrm{PSD95}} = 0.055$/h). We defined 1 relative intensity unit (RIU) as the mean band density on immunoblotting from net production of PSD95 in 4 h. By immunoblotting lysates from cells incubated for 24 h with ASV then for 4 h without ASV, we obtained a protein amount of 1 RIU for $[\mathrm{PSD95}]_{(4\ \mathrm{h})}$ (s.d. 0.16, $n = 3$). By immunoblotting in parallel lysates from cells incubated for 24 h without ASV then for 4 h with ASV, we obtained a protein amount of 0.419 RIU for $[\mathrm{PSD95SMASh}]_{(4\ \mathrm{h})}$ (s.d. 0.07, $n = 3$). With values for $k_{\mathrm{deg,\ PSD95}}$ and for $[\mathrm{PSD95}]_{(4\ \mathrm{h})}$, we then used equation 3 to solve numerically for $k_{\mathrm{syn,\ PSD95}}$, obtaining 0.279 RIU/h. Assuming $k_{\mathrm{syn,\ PSD95SMASh}}$ equals $k_{\mathrm{syn,\ PSD95}}$, we could then use equation 4 to solve numerically for $k_{\mathrm{deg,\ PSD95SMASh}}$, obtaining 0.606/h. The PSD95-SMASh half-life $t_{1/2,\ \mathrm{PSD95SMASh}}$ was then calculated as 1.14 h ($t_{1/2,\ \mathrm{PSD95SMASh}} = \ln_2/k_{\mathrm{deg,\ PSD95SMASh}} = 1.14$ h).

The half-life of CYP21A2-SMASh was calculated from the same equations, except CYP21A2 was substituted for PSD95. Values obtained were: $t_{1/2,\ \mathrm{CYP21A2}} = 2.4$ h, $k_{\mathrm{deg,\ CYP21A2}} = 0.288$/h, $[\mathrm{CYP21A2}]_{(4\ \mathrm{h})} = 1$ RIU (s.d. 0.019, $n = 3$), $[\mathrm{CYP21A2SMASh}]_{(4\ \mathrm{h})} = 0.163$ RIU (s.d. 0.025, $n = 3$), $k_{\mathrm{syn,\ CYP21A2}} = k_{\mathrm{syn,\ CYP21A2SMASh}} = 0.422$/h, $k_{\mathrm{deg,\ CYP21A2SMASh}} = 2.688$/h, $t_{1/2,\ \mathrm{CYP21A2SMASh}} = 0.258$ h.


51. Thomas, B.J. & Rothstein, R. Elevated recombination rates in transcriptionally active DNA. *Cell* **56**, 619–630 (1989).
52. Brindley, M.A. *et al.* A stabilized headless measles virus attachment protein stalk efficiently triggers membrane fusion. *J. Virol.* **87**, 11693–11703 (2013).
53. Buchholz, U.J., Finke, S. & Conzelmann, K.K. Generation of bovine respiratory syncytial virus (BRSV) from cDNA: BRSV NS2 is not essential for virus replication in tissue culture, and the human RSV leader region acts as a functional BRSV genome promoter. *J. Virol.* **73**, 251–259 (1999).
54. Krumm, S.A., Takeda, M. & Plemper, R.K. The measles virus nucleocapsid protein tail domain is dispensable for viral polymerase recruitment and activity. *J. Biol. Chem.* **288**, 29943–29953 (2013).
55. Ono, N. *et al.* Measles viruses on throat swabs from measles patients use signaling lymphocytic activation molecule (CDw150) but not CD46 as a cellular receptor. *J. Virol.* **75**, 4399–4401 (2001).
56. Plemper, R.K., Hammond, A.L., Gerlier, D., Fielding, A.K. & Cattaneo, R. Strength of envelope protein interaction modulates cytopathicity of measles virus. *J. Virol.* **76**, 5051–5061 (2002).






doi:10.1038/nchembio.1869